

since $S(b',b)$ is the probability for an atom to make an rf transition from (b') to (b) . When the rf is applied the population of (b) is changed to

$$[1-S(b,b')][E(b,a)]+[S(b',b)][E(b',a)]. \quad (15)$$

A similar expression holds for the population of (b') . $D(b,c)$ is the probability of an atom decaying from (b) to a final ground state (c) . Therefore the change in $W(c,a)$ produced by the rf is $\Delta W(c,a)$, where

$$\Delta W(c,a) = \{[D(c,b)][-E(b,a)+E(b',a)] + [D(c,b')][-E(b',a)+E(b,a)]\} \{S(b,b')\}, \quad (16)$$

and we have used $S(b,b')=S(b',b)$. Equation (16) reduces to

$$\Delta W(c,a) = [D(c,b)-D(c,b')][E(b',a)-E(b,a)] \times \left[\frac{V^2}{2[V^2+G^2+(f-f_0)^2]} \right]. \quad (17)$$

The total relative excited state rf effect ΔW is

$$\Delta W = \sum_{c'} aW(c,a), \quad (18)$$

where the summation is over all initial states (a) and those final states (c') which have a value of m_J which is different from the m_J value of the initial state (a) . This is the same type of summation as the one described in Sec. A of Appendix 1 in the calculation of the total relative light effect. The ratio of the excited state rf effect to the light effect, which is the quantity of experimental interest, is simply $(\Delta W)/L$.

Equation (17) shows that ΔW depends on the optical matrix elements connecting (b) and (b') to the ground state levels. It is this dependence which leads to wide variation in the intensities of the excited state rf effects between different pairs of excited state levels. From Eq. (14), the width of the excited state rf effect resonance curve at half-intensity is g , where

$$g^2 = k^2 + V^2. \quad (19)$$

Photoprotons from Lead-208 and Tantalum*

M. ELAINE TOMS† AND WILLIAM E. STEPHENS

Physics Department, University of Pennsylvania, Philadelphia, Pennsylvania

(Received December 23, 1954)

The photoprotons ejected from thin foils of tantalum and enriched lead-208 by the 23-Mev bremsstrahlung x-rays from a betatron have been observed in nuclear emulsions. Yields, measured in units of 10^4 protons per mole per roentgen unit, are: tantalum, 5.6 ± 0.5 ; lead-208, 2.6 ± 0.3 . The angular distribution of the lead-208 protons shows a strong forward asymmetry while the tantalum protons are more isotropic. Both proton energy distributions are in good agreement with the predictions of the direct photoprocess.

PREVIOUS work^{1,2} has shown that the Coulomb barrier in heavy elements ($Z > 40$) strongly inhibits the emission of "evaporated" photo protons. Many of the photoprotons that are observed are ascribed to a direct photoeffect.^{1,3} We have extended these measurements to the photoprotons from tantalum and lead enriched in isotope 208.⁴

Using the techniques described previously,^{1,5-7} Ilford E-1 200-micron plates were placed in an evacuated "camera" to detect charged particles ejected from thin foils by collimated x-rays from the University of Pennsylvania betatron run at 23 Mev. The plates were de-

veloped by the temperature change method and later scanned. The track ranges were corrected by adding half the effective foil thickness and converted to photon energies. Table I gives the details of the two runs.

The energy distributions of the photoprotons are shown in Figs. 1 and 2. The tracks between 2 and 5

TABLE I. Exposure details.

	Tantalum	Lead-208
Foil thickness (mg/cm ²)	16.6	21.8
(mils)	0.4	0.75
Effective half-thickness for 10-Mev protons (Mev)	0.16	0.2
Purity	0.99+	0.966
X-ray exposure (roentgens)	28 950	27 850
Area scanned (cm ²)	2.1	2.2
Protons measured	414	231
Alphas observed	2	2
Estimated proton background	40±16	44±16
Proton tracks observed in background region (2-5 Mev)	20	20
Yields:		
(10 ⁴ protons mole ⁻¹ roentgen ⁻¹)	5.6±0.5	2.6±0.3
(10 ⁴ alphas mole ⁻¹ roentgen ⁻¹)	0.003±0.02	0.04±0.03

* Supported in part by the joint program of the Office of Naval Research and the U. S. Atomic Energy Commission.

† Now at the Naval Research Laboratory, Washington, D. C.

¹ M. E. Toms and W. E. Stephens, Phys. Rev. **92**, 362 (1953).

² E. V. Weinstock and J. Halpern, Phys. Rev. **94**, 1651 (1954).

³ E. D. Courant, Phys. Rev. **82**, 703 (1951).

⁴ We are indebted to the Isotopes Division of the U. S. Atomic Energy Commission for the loan of the enriched lead.

⁵ M. E. Toms and W. E. Stephens, Phys. Rev. **82**, 709 (1951).

⁶ P. R. Byerly and W. E. Stephens, Phys. Rev. **83**, 54 (1951).

⁷ M. E. Toms and W. E. Stephens, Phys. Rev. **95**, 629(A) (1954).

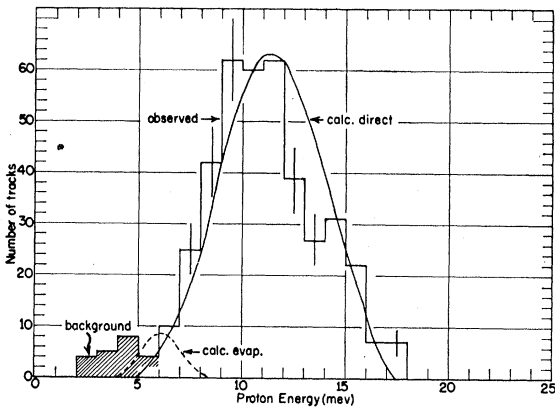


FIG. 1. The histogram gives the energy distribution of the photoprotons from tantalum exposed to 23-Mev bremsstrahlung. The smooth curve is the distribution calculated for the direct process and normalized to the observed protons. The dashed curve is the calculated distribution for the evaporation process fitted to indicate the maximum possible evaporation yield. The shaded groups are background.

Mev which are shaded in the figures are ascribed to background as determined in a previous exposure.¹ The yields corrected for these backgrounds are given in Table I.

The photoproton angular distributions are plotted in Figs. 3 and 4 both for all the p otons and for various energy groups.

DISCUSSION

The observed photoproton energy distributions are shown as histograms in Figs. 1 and 2 and can be compared with theoretical calculations. The solid curves of Figs. 1 and 2 are the distributions predicted by a direct photoeffect calculated as in our previous work.¹ The theoretical curves are fitted to the histograms and show good agreement. The distributions expected from an

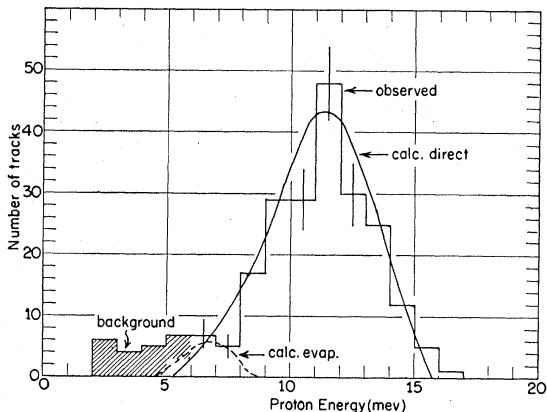


FIG. 2. The histogram gives the energy distribution of the photoprotons from lead 208 exposed to 23-Mev bremsstrahlung. The smooth curve is the distribution calculated for the direct process and normalized to the observed protons. The dashed curve is the calculated distribution for the evaporation process fitted to indicate the maximum possible evaporation yield. The shaded groups are background.

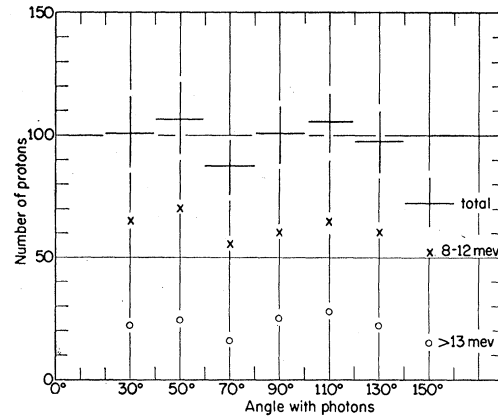


FIG. 3. The numbers of tantalum photoprotons per unit solid angle in arbitrary units is plotted as a function of their angle from the photon direction. In addition, the crosses show the angular distribution of photoprotons of 8 to 12 Mev energy, the circles photoprotons over 13 Mev.

evaporation process are shown as dotted curves in Figs. 1 and 2, fitted somewhat arbitrarily to show the maximum evaporation yield which reasonably could be consistent with the observed protons. There is, in fact, no evidence for evaporated protons as such.

The yields to be expected from the direct and evaporation processes are calculated and tabulated in Table II together with the observed values. The "Possible obs. evap." yields, given in row eleven of Table II, are determined by the number of observed photo protons in the energy region predicted by the evaporation process. Since this energy region overlaps that for the direct process, positive identification is not possible. Table II

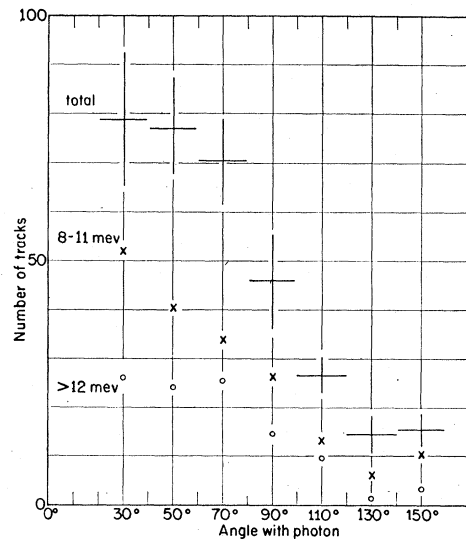


FIG. 4. The numbers of lead-208 photoprotons per unit solid angle in arbitrary units is plotted as a function of their angle from the photon direction. In addition, the crosses show the angular distribution of photoprotons of 8 to 11 Mev energy, the circles photoprotons over 12 Mev.

TABLE II. Calculated and observed photoproton yields.

	Bi	Pb ²⁰⁸	Ta	Ce	In	Mo ¹⁰⁰	92
Z protons	83	82	73	58	49	42	
B_p (Mev) ^a	3.76	8.02	6.2	8.5	6.8	10.5	8.0
N neutrons	126	126	108	82	66	58	50
B_n (Mev) ^a	7.44	7.38	7.55	7.05	9.05	8.1	13.1
Y_p (observed)	5	2.6	5.6	12	11.7	9.2	160
(10 ⁴ protons mole ⁻¹ roentgen ⁻¹)				($\lesssim 9$ direct)	($\lesssim 8$ direct)		
Betatron energy (Mev)	24	23	23	23	24	22.5	22.5
Y_p (calc. direct)	1.5	0.2	0.7	0.7	2		
(10 ⁴ protons mole ⁻¹ roentgen ⁻¹)							
Y_p (obs.)/ Y_p (calc. direct)	3.3	13	8	13	4		
Y_p (calc. evap.)	0.3	0.002	0.05	0.07	1.1	0.6 to	120 to
(10 ⁴ protons mole ⁻¹ roentgen ⁻¹)						0.37	220
Y_p (obs.)/ Y_p (calc. evap.)	17	1300	110	170	10	125 to	~ 1
						20	
Possible obs. evap.	<0.3	<0.2	<0.2	<3	<3	forward ^d	\sim isotr. ^d
Angular distr.	far forward ^b	far forward ^c	\sim isotr. ^c	\sim isotr. ^b	forward ^b		

^a B_p is the binding energy of the last proton; B_n is the binding energy of the last neutron.

^b M. E. Toms and W. E. Stephens, Phys. Rev. 92, 362 (1953).

^c Present work.

^d W. A. Butler and G. M. Almy, Phys. Rev. 91, 58 (1953).

also contains data on other heavy elements which have been previously reported.

The observed yields of protons whose energies are appropriate to the direct photoeffect vary from about 4 to 13 times the values predicted by Courant's direct effect. Factors of this order of magnitude can be accounted for by including a wine bottle potential and an alpha-particle structure⁸ in the direct-effect calculations. A similar increase is predicted by Wilkinson⁹ who suggests that the nuclear photoeffect is primarily the excitation of a nuclear particle from a closed shell to a single-particle level. A "pseudo-direct" process would result if this particle is emitted before interacting further with the rest of the nucleus. Wilkinson calculates that this pseudo-direct process should be 20 to 60 times as probable as Courant's direct photoeffect (this factor may be less because the resultant nucleus must be left in a suitable state).

As indicated in Table II, the observed photoprotons are 10 to 1300 times as abundant as the evaporation process would predict. This disparity in yields and the difference between the observed proton energies and the evaporated predicted energy distribution show clearly the impossibility of accounting for the photoprotons by the evaporation model and confirms our previous conclusion that the protons are caused by a direct photoeffect.

The few protons of energy greater than 15 Mev from lead may come from the small amount of lead 207 (2.3 percent) and 206 (1 percent) which were present in the enriched lead 208 foil. The few alpha particles

observed are not inconsistent with evaporation both in yield and energy.

The angular distributions shown in Figs. 3 and 4 are somewhat surprising. The direct photoeffect with dipole absorption should give angular distributions which are symmetric around 90°. Even quadrupole absorption with its interference effects can contribute to forward asymmetries with a peak only as far forward as 45°. It is not clear whether the high experimental points forward of 45° are reliable enough to require octupole absorption.

The specificity of the forward asymmetry suggests a nuclear shell-structure effect. Varying amounts of forward asymmetry may be caused by a dipole-quadrupole (or higher multipole) interference due to various relative positions of the "resonances" for the various multipole absorptions from nucleus to nucleus depending on the nuclear structure. This may not necessarily depend directly on the last proton shell since the high centrifugal barrier for large l may inhibit the last proton from exhibiting a "pseudo-direct" effect as proposed by Wilkinson.⁹ It is tempting to point out that lead 208 and bismuth are considered to have a low l shell ($3s$) near or at the top of the proton shell. In these cases, a "pseudo-direct" effect as suggested by Wilkinson may be possible and if the quadrupole resonance (small compared to the dipole resonance) happens to occur on the high-energy tail of the dipole resonance, above the Coulomb barrier, the interference will enhance the forward asymmetry of the protons observed. However, it is not certain that there may not be some mechanism operating other than those we have suggested.

⁸ D. H. Wilkinson, Proceedings of the Photonuclear Conference at University of Pennsylvania, May 3, 1954 (unpublished).

⁹ We are indebted to Dr. D. H. Wilkinson for his discussion of this effect.